Electrochimica Acta 144 (2014) 64–70

Contents lists available at ScienceDirect

Electrochimica Acta

journal homepage: www.elsevier.com/locate/electacta

Plasmonic versus catalytic effect of gold nanoparticles on mesoporous TiO_2 electrodes for water splitting

Marta Haro[a], Rafael Abargues[b,c], Isaac Herraiz-Cardona[a], Juan Martínez-Pastor[b], Sixto Giménez[a,*]

[a] Photovoltaics and Optoelectronic Devices Group, Departament de Física, Universitat Jaume I, 12071 Castelló, Spain
[b] UMDO, Instituto de Ciencia de los Materiales, Universitat de València, P.O. Box 22085, 46071 Valencia, Spain
[c] Intenanomat S.L. C/Catedrático José Beltrán 2, 46980 Paterna, Spain

ARTICLE INFO

Article history:
Received 2 June 2014
Received in revised form 23 July 2014
Accepted 28 July 2014
Available online 13 August 2014

Keywords:
Water splitting
photoelectrochemistry
plasmonics
catalysis
TiO2

ABSTRACT

Solar water splitting with metal oxide semiconductors constitutes a promising approach to the conversion of solar energy into chemical energy stored in the atomic bonds of hydrogen molecules. In the present study, we evaluate the effect of the presence of Au nanoparticles on the photoelectrochemical behaviour of mesoporous TiO_2 to photo-oxidize water. We observe that the presence of Au nanoparticles leads to enhanced photocurrents for water oxidation and we explore the origin of this enhancement by optical and electrochemical characterization techniques. Our results indicate that although the Au nanoparticles are responsible for a localized surface plasmonic resonance effect, which significantly improves the optical density of the electrodes, the main contribution of these nanoparticles to the photocurrent has a catalytic origin as evidenced by the faster charge transfer kinetics.

1. Introduction

The need to revolutionize the way energy is produced, delivered, and utilized is widely recognized. Due to an increasing population and rising living standards around the globe, the need for a reliable, convenient, and adaptable energy supply is increasing. As a clean fuel, hydrogen is very attractive due to its high energy density and benign chemical byproduct, which can be produced from water and sunlight.[1] To accomplish this artificial photosynthesis, an economically viable water splitting cell requires good electrode stability in aqueous solutions under harsh conditions, appropriate positions of the conduction and valence band energy levels respect to required reaction potentials, good visible light efficiency, efficient charge carrier separation and transport, and facile interfacial charge-transfer. To date, no single material has fulfilled all the required conditions. Recent advances in nanotechnology and catalysis, however, greatly increase the prospects for developing a combination of materials capable of efficient conversion of sunlight to chemical fuels.[2]

Since Honda and Fujishima's electrochemical photolysis report using TiO_2, [3] intensive efforts have been dedicated to improve photoelectrochemical cells (PECs) based on this material. It has attracted significant attention due to its low cost, easy preparation, high stability in aqueous solution under oxygen-evolving conditions. Furthermore, since the valence band of TiO_2 lays well below the H_2O/O_2 potential, spontaneous transfer of holes to the H_2O molecules takes place, driving the oxidation half-reaction forward. While TiO_2 is one of the most promising photocatalysts, its main drawback is related to its negligible absorption in the visible region of the electromagnetic spectrum, then only ca. 4% of the solar photons can be used to drive the water splitting process. In any case, this system appears as an excellent platform to study and understand new optoelectronic effects, which could be applied to enhance the functional performance of photoelectrochemical devices.

Over the past several years, the use of gold nanoparticles (NPs) prepared on various transition metal oxides has emerged as a promising new strategy for improving the efficiency of photocatalytic processes. Contrary to the poor catalytic activity of bulk gold, unique catalytic properties have been described when Au is in the form of nanoparticles.[4,5] Moreover, gold at the nanoscale exhibit Localized Surface Plasmon Resonance (LSPR), consisting of the collective oscillations of the conducting electrons confined to the surface generating an intense electric field upon irradiation at its LSPR frequency. This resonance frequency can be tuned by controlling the nanoparticle size, shape, material, and proximity to other

* Corresponding author.
E-mail address: sjulia@uji.es (S. Giménez).

http://dx.doi.org/10.1016/j.electacta.2014.07.146
0013-4686/

NPs,[6] opening a wide avenue of possibilities for optoelectronic, photoelectrochemical and photocatalytic applications.

Regarding photocatalysis, the presence of gold NPs on the surface of semiconductor metal oxides can increase the electron-hole pair separation, since the photogenerated electrons can be "captured" by a noble metal, provided that its work function is placed at lower energy than the conduction band edge of the semiconductor. In this situation, since electrons accumulate at the Au NP, their Fermi level shifts to more negative values, approaching to the CB edge of the semiconductor.[7–10] The storage of electrons has been observed through a blue-shift in the LSPR frequency.[11] This energy alignment for the semiconductor-Au NPs promotes the charge transfer and thereby increases the lifetime of photogenerated electrons and holes, enhancing the photocatalytic water oxidation since it is a slow multielectron process with kinetic limitations.

On the other hand, there are studies reporting the decrease of the photocatalytic activity of metal oxides (such as CeO_2 and TiO_2 with Au) when these electrodes were irradiated with bandgap illumination, suggesting that gold NPs act as electron-hole recombination centers. Meanwhile, upon visible illumination the photocatalytic response increases due to the contribution of the LSPR.[12–14] The increase of photocurrent in the visible region has been extensively ascribed to the electron transfer from the gold NPs to the semiconductor.[15–17] In this model, the gold NPs are photoexcited due to LSPR, and charge separation is accomplished by the transfer of photoexcited electrons from the Au NP to the conduction band of the metal oxide substrate.[18] The main drawback of this model is that LSPR consists of the electron gas oscillation at the metal NP, and it does not exist valence-conduction band energy separation associated to this nanomaterial. The plasmonic charge resides at the Fermi energy of the metal, and it is neither able to drive the reduction nor oxidation half-reactions.[19] Recently, the photocurrent increase in the visible region has been explained by "local hot spots", where the electric field intensity that reaches the TiO_2 surfaces is 1000 times higher compared to the incident electric field due to the coupling between the incident light and the LSPR.[13,20–22] Moskovits el al. explained this charge transfer mechanism, in which the LSPR decay produces electron-hole pairs in the gold and the resulting hot electrons are, then, directly injected into TiO_2 by quantum tunneling.[23,24] In this line, Snaith [25] and Konstantatos [26] have observed the electron injection from metallic NPs to the semiconductor through an insulator layer.

Considering the controversial influence of noble metals on the photoactivity of metal oxide semiconductor materials, the present study aims at understanding whether the LSPR and the catalytic properties of nano-gold effectively enhance the photo-dissociation of water to produce hydrogen and oxygen. For this purpose, mesoporous TiO_2 electrodes with different amounts of embedded Au NPs have been synthesized. We have carried out a detailed structural and photoelectrochemical characterization of these electrodes. The obtained results show that Au NPs exhibit LSPR effect, which is not efficiently translated into a photocurrent. On the other hand, the presence of these Au NPs significatively enhances the catalytic behavior of the electrodes, as reflected on the faster charge transfer kinetics, compared to reference electrodes.

2. Materials and methods

2.1. Electrode preparation

TiO_2 nanoparticulated films were deposited by screen-printing a commercially available colloidal paste (Dyesol 18 NT) on transparent conducting fluorine doped tin oxide (FTO) glass substrates (TEC 15 Pilkington TEC GlassTM, sheet resistance ca. 10 Ω cm). The FTO substrates were previously cleaned with detergent and de-ionised water, followed by sonication in isopropanol and ozone treatment. The resulting films were sintered at 450 °C in order to achieve good electrical contact between the nanoparticles. The thickness of the as-prepared TiO_2 films was approximately 5 μm measured by a Dektak 6 profilometer from Veeco.

Au NPs were *in situ* synthesized into the TiO_2 mesoporous film through an ionic adsorption and thermal-reduction approach. Briefly, 100 μl of a solution of 5 mM $HAuCl_4$ in ethanol were dropped onto the TiO_2 film. After 60 seconds, the substrate was spin-coated at 1000 rpm for 30 s and then baked in a hot plate at 60 °C for 30 seconds and at 200 °C for 10 minutes. The Au(III) ions were reduced to metallic Au NPs and a color change from white to light violet of the film can be observed. Increasing the number of Au deposition cycles can enhance the amount of Au NPs into the TiO2 film. The samples are labeled as TiO2@Au-n, where n is the number of deposition cycles of the Au solution onto the TiO_2 mesoporous film.

2.2. Optical, structural, morphological and electrochemical characterization

The UV-vis spectra were recorded by a Cary 500 UV-VIS Varian photospectroscometer between 300 nm and 900 nm. Incident photon to converted electron (IPCE) measurements of the samples was performed in the PEC cell with an applied bias of 1 V vs RHE and illuminating with a 150 W Xe lamp coupled with a monochromator controlled by a computer. The light intensity was measured using an optical power meter 70310 from Oriel Instruments where a Si photodiode was used to calibrate the system. Current density voltage (*j-V*) and electrochemical impedance spectroscopy (EIS) measurements were carried out using a FRA equipped PGSTAT-30 potetiostat from Autolab. A three-electrode configuration was used, where a Pt wire and a Ag/AgCl electrodes were used as counter-electrode and as reference electrode, respectively. The electrolyte was a 1 M NaOH solution (pH = 13). The electrodes (geometrical area 1 cm^2) were illuminated using a 300 W Xe lamp, where the light intensity was adjusted with a thermopile to 100 mW cm^{-2}. EIS measurements were carried out by applying a 20 mV AC signal and scanning in a frequency range between 100 kHz and 50 mHz, at different applied bias. All potentials have been referred to the Reversible Hydrogen Electrode (RHE) by the expression: $V_{RHE} = V_{Ag/AgCl} + 0.210 + 0.059 \cdot pH$. The numerical fitting of the impedance data was carried out using the Zview software (Scribner Associates).

3. Results and Discussion

The synthesis of Au NPs into the mesoporous TiO_2 film is based on the adsorption of $[AuCl_4]^-$ in the TiO_2 film and the subsequent thermal decomposition during the bake step. Fig. 1 shows representative SEM micrographs of the cross-section (Fig. 1a) and top- view (Fig. 1b) of a film of TiO_2 embedded with Au NPs after 4 deposition cycles of Au(III) solution (5 mM). Surface inspection reveals microstructure formed by round-shaped nanograins of TiO_2. At this magnification, the Au nanoparticles cannot be observed, and the film microstructure and morphology observed are identical to those for reference pristine TiO_2 electrodes. However, EDS microanalysis clearly confirms the presence of Au (See Supporting Information, Figure SI1). Moreover, XRD clearly shows the characteristic diffraction peaks corresponding to TiO_2 and Au (Fig. 1c). The crystal size of TiO_2 and Au was calculated from XRD peaks corresponding to (101) and (111) planes of TiO_2 and Au, respectively, using the Scherrer formula. The estimated crystallite size of TiO_2 and Au nanoparticles is 15.0 ± 0.6 nm and 9.0 ± 0.3 nm,

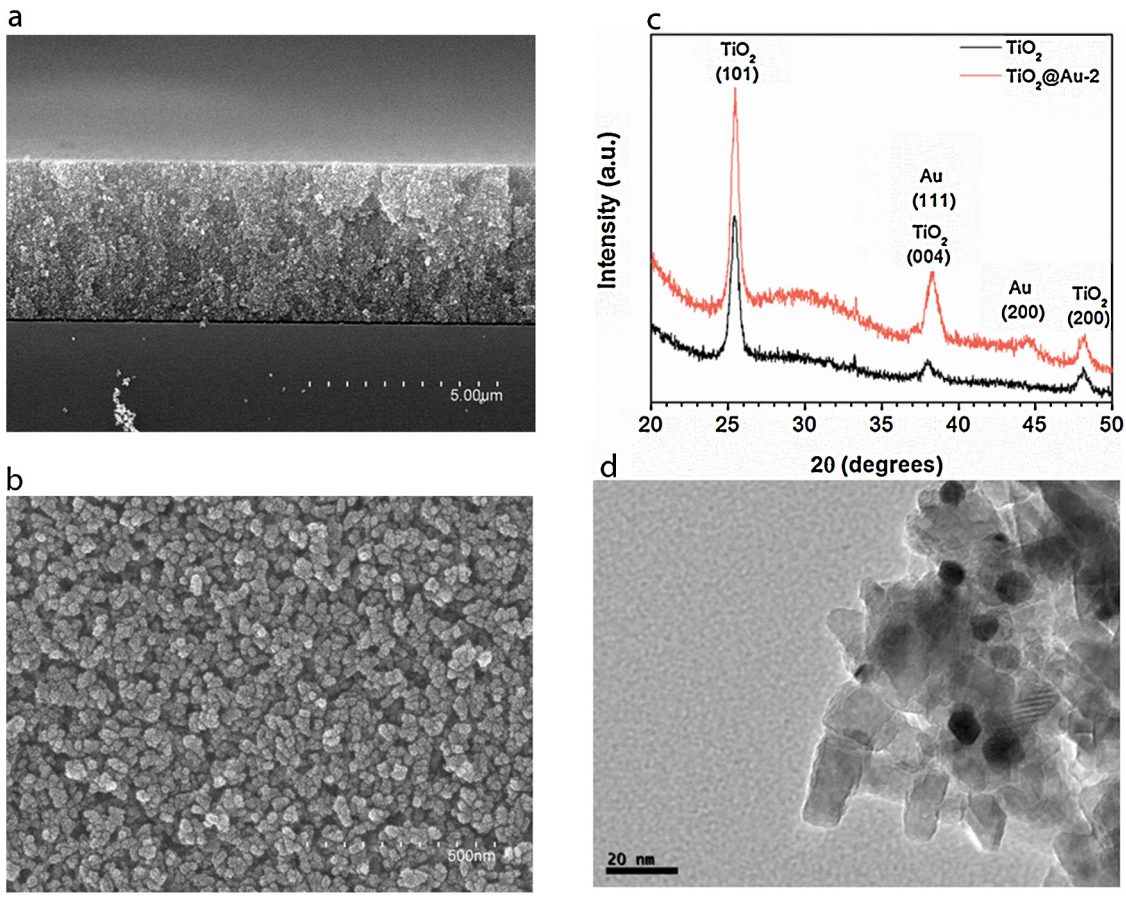

Fig. 1. Film of TiO_2 with Au nanoparticles obtained after 4 cycles of spin-coating (a) Cross-section and (b) Top-view obtained by SEM. (c) XRD diffractogram and comparison with a reference TiO_2 electrode. (d) Representative TEM image of a TiO_2 with Au nanoparticles obtained after 4 cycles of spin-coating. The Au nanoparticles are clearly visible showing increased contrast.

respectively. TEM measurements confirmed the spherical morphology of the Au NPs and a narrow size distribution around 8-9 nm (Fig. 1d).

Fig. 2 shows the UV-Vis absorbance spectra of TiO_2 mesoporous films embedded with Au NPs prepared from different Au deposition cycles. All the films show a symmetric band centered at 548 nm, which is attributed to Au NPs. Above two deposition cycles, the LSPR band intensity increases linearly with the number of deposition cycles (see the inset at Fig. 2). The LSPR peak wavelength does not shift with the number of deposition cycles of Au, due to the similar size of the NPs. We also observe that LSPR bands are symmetric, which indicates that Au NPs are homogeneously dispersed into the mesoporous film and interparticle spacing among Au NPs is large enough to avoid plasmon coupling.[6] These two facts suggest that the ionic adsorption of Au into the TiO_2 mesoporous film is not saturated after 4 deposition cycles. Additionally, the observation of the LSPR effect on Au nanoparticles indirectly evidence the 0-oxidation state of Au.

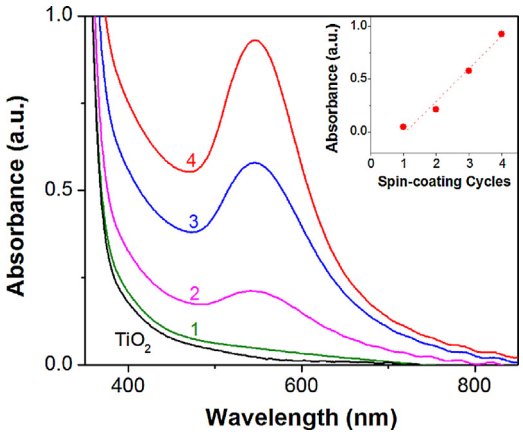

Fig. 2. UV-vis spectra of the pristine TiO_2 and TiO_2@Au films. The number of spin-coating cycles of the Au solution onto the TiO_2 film is indicated. The maximum absorbance of the plasmon at 548 nm versus the number of spin-coatings is represented in the inset.

The photoelectrochemical performance of Au decorated TiO_2 photoelectrodes was studied through three-electrode measurements in the dark and under illumination. Fig. 3(a) shows representative *j-V* curves of a TiO_2 electrode embedded with Au NPs in the dark and under illumination at 100 $mW{\cdot}cm^{-2}$. The dark *j-V* curve shows a large potential range where current does not flow through the electrochemical cell, with a cathodic current below 0.4 V *vs RHE* related to the O_2 reduction to OH^- molecules. The cathodic peak observed at 0.02 V *vs RHE* is related to the electron transfer through a localized interbandgap TiO_2 state, in agreement with previous studies.[27–29] This cathodic peak is less pronounced under illumination, consistently with the presence of photogenerated holes, which recombine with electrons located at surface states. Additionally, a positive photocurrent is observed under illumination due to photogenerated holes injected in the solution. The evolution of the plateau photocurrent with the Au NP loading does not show a monotonic behavior as showed in the inset of Fig. 3 (b). This volcano-type relationship between the loading amount of Au NPs and the photocalytic activity is

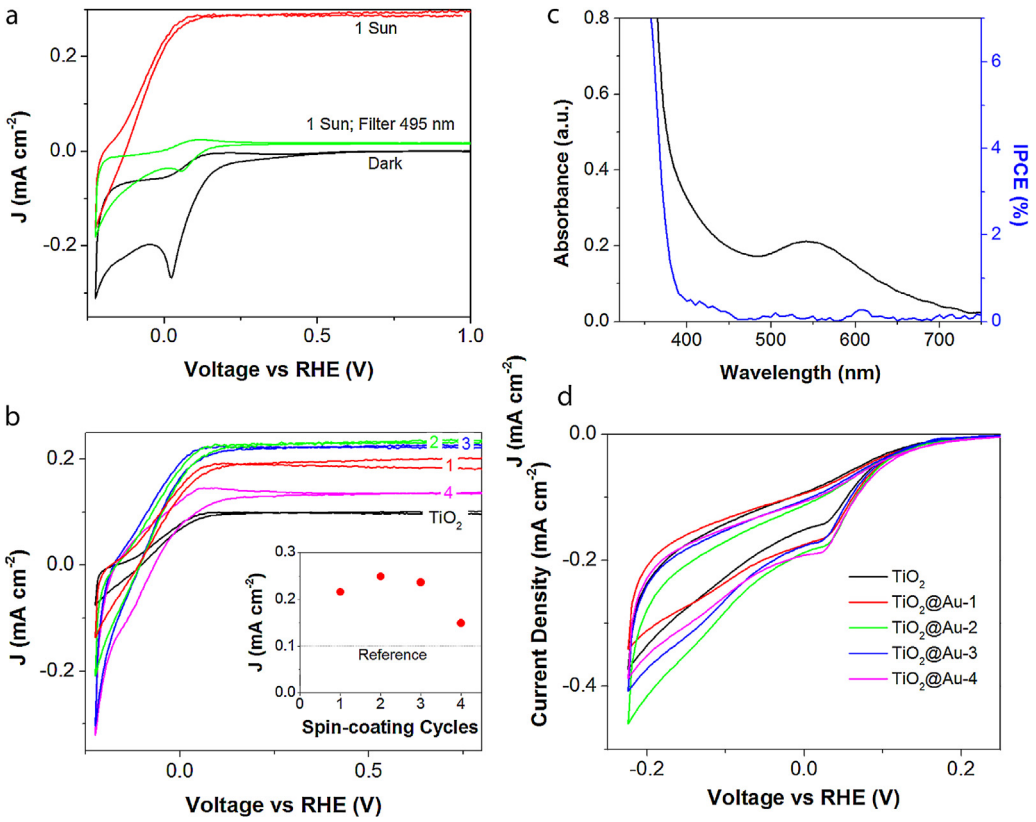

Fig. 3. (a) *j-V* curves of a representative sample TiO_2@Au under illumination without filter and with a cut-off filter of 495 nm. (b) *j-V* curves under illumination of mesoporous pristine TiO_2 (as a reference) and with different loading of embedded Au NPs (the number of spin-coating cycles for each curve is indicated). Inset figure, photocurrent at V = 1 V *vs RHE* versus the number of spin-coatings of the loading Au NPs on the TiO_2 electrodes. (c) Absorbance and IPCE of the TiO_2@Au-2 sample. It is clear that no photocurrent is generated at the wavelengths where the plasmonic resonance takes place. Identical behavior has been systematically observed for the different Au loadings tested. (d) j-V curves in the dark of TiO_2@Au samples. We only show the voltage region where charge injection from the solution to TiO_2 takes place.

the typical behavior of cocatalysts deposited on semiconductor electrodes.[30] The decrease of the photocatalytic activity after an optimal cocatalyst-semiconductor ratio has been ascribed to several factors: i) coverage of the surface active sites of the semiconductor, ii) screening of the incident light, iii) increase of the cocatalyst size (albeit this factor can be ruled out by the TEM, UV-vis and X-ray data), and iv) high loading amount of cocatalyst can act as charge-recombination centers.

In order to understand the origin of the photocurrent enhancement due to the presence of Au NPs embedded in the mesoporous TiO_2 photoanode, *j-V* curves under illumination were obtained by placing a 495 nm cut-off filter between the light source and the sample in order to eliminate the contribution of TiO_2 to the photoresponse. A representative example is included in Fig. 3a showing the characteristic peak of electron transfer through localized surface states at 0.02 V *vs RHE* and a very low photocurrent of ca. 20 $\mu A\,cm^{-2}$. This result clearly indicates that the plasmonic effect of the gold NPs in these samples hardly contributes to the overall increase of the photocurrent. Moreover, the external quantum efficiency (EQE) of these electrodes was evaluated through Incident Photon to Current Efficiency (IPCE) measurements (Fig. 3c) and no enhancement was observed at the plasmonic frequency for all tested samples. On the other hand, the dark *j-V* curves systematically show higher injection currents for Au decorated films, as showed in Fig. 3(d) indicating that Au nanoparticles play a catalytic role on the charge transfer between TiO_2 and the aqueous solution.

Further information on the carrier dynamics of mesoporous TiO_2 photoanodes with embedded gold NPs was extracted by electrochemical impedance spectroscopy (EIS) measurements in the dark and under illumination. Previous investigations of EIS to elucidate the traffic of carriers at the mesoporous TiO_2/solution interface highlighted the key role of surface states on the electrode kinetics and the coupling of transport and charge transfer processes since the reactive surface is distributed along the whole film thickness. Consequently, we have applied the well-established transmission line model, which allows the comprehensive understanding of the electron dynamics (Fig. 4a and 4b).[29] The parallel C_{FTO} capacitance with the transmission line accounts for the interfacial capacitance between FTO and the electrolyte, when charge transfer through the FTO is blocked. Representative Nyquist plots of the mesoporous TiO_2 electrodes without and with embedded Au NPs at V = 27 mV *vs RHE* are shown in Fig. 4(c). At this potential, the measured spectra are characterized by an arc closing at low frequencies, related to the chemical capacitance of TiO_2 (C_μ) and charge transfer resistance (R_{ct}). At high frequencies, a clear 45 degrees straight line is observed, which is related to electron diffusion through the mesoporous film (R_{tr}).[31] A magnification of the high frequency region of the Nyquist plot is showed as Fig. 4(d). When Au NPs are embedded in the mesoporous TiO_2 electrodes, the shape of the Nyquist plots is identical but some differences can be observed. At 27 mV *vs RHE*, Figs. 4(a) and 4(b), both charge transfer resistance and transport resistance are lower when Au NPs are present, indicating that Au enhances both water oxidation catalysis and electron transport within the electrode.

Representative values of the parameters extracted from fitting the EIS data under illumination for different loadings of Au NPs are collected in Fig. 5 as a function of applied bias. Additionally, information of a reference pristine TiO_2 sample is included for comparison. Similar behavior was obtained for measurements in the dark, which are showed as Supporting Information, Figure SI2.

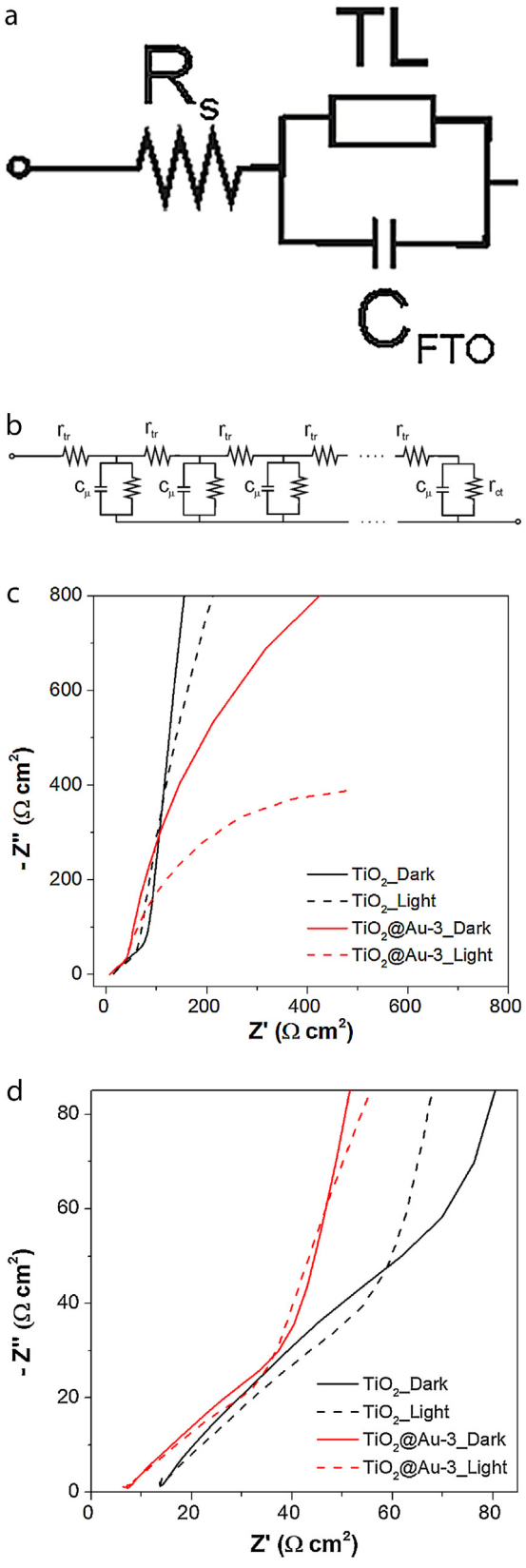

Fig. 4. (a) Simplified equivalent circuit used to fit the impedance spectra, (b) Description of the transmission line (TL) element. (c) EIS spectra obtained at 27 mV *vs RHE* in the dark and under 100 mW·cm^{-2} illumination. (d) Magnification of the squared area in (c) to illustrate the 45° line related to electron transport resistance.

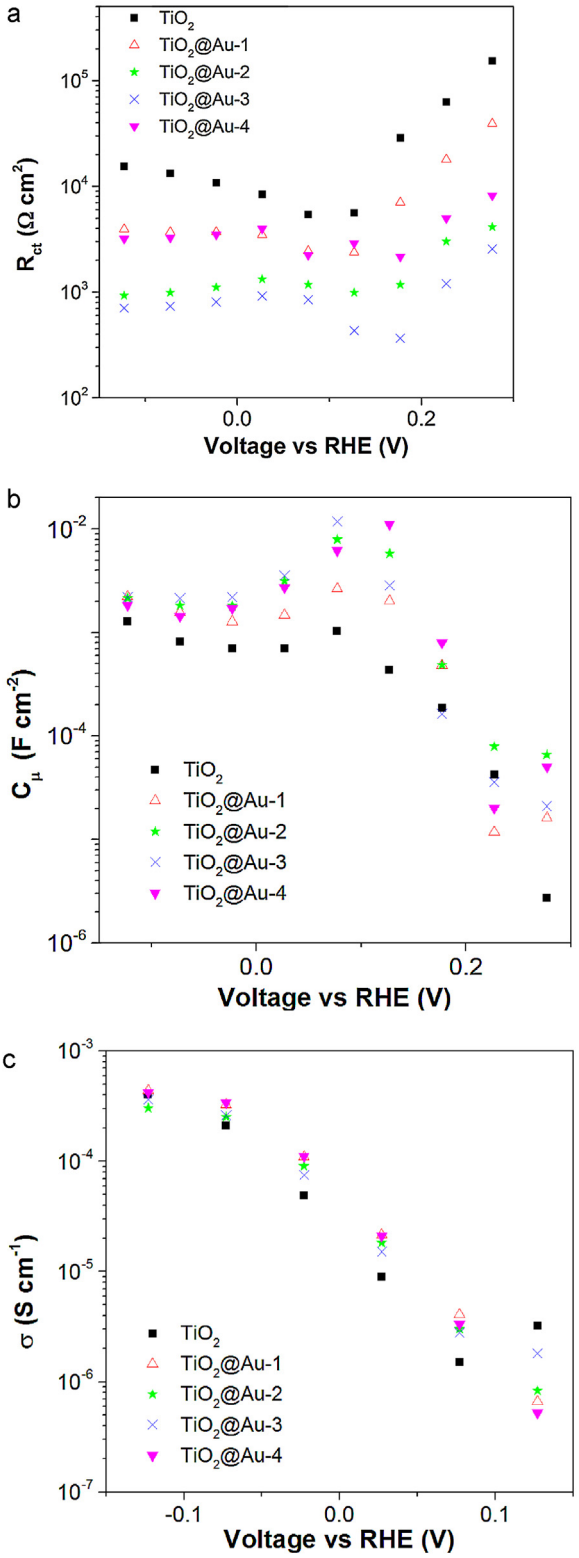

Fig. 5. (a) Chemical capacitance, (b) charge transfer resistance, and (c) conductivity of mesoporous TiO_2 films without and with different loading of Au NPs under illumination at 100 mW·cm^{-2}. The conductivity has been only calculated in the potential range where the transmission line is observed.

Since the measured currents are below 1mA·cm^{-2} in all measured samples, the correction for ohmic losses is negligible and it has been omitted in the present study. The exponential evolution of capacitance with voltage (Fig. 5a) clearly reflects the density of interbandgap states near the conduction band of TiO_2. We observed that TiO_2 films containing Au NPs show higher values of chemical capacitance, which may arise from the increased density of states due to Au NPs.[32] The capacitance peak around 0.1 V vs RHE accounts for the presence of the monoenergetic surface state, consistently with the reduction peaks observed by cyclic voltammetry in Fig. 3. Additionally, the charge transfer resistance (Fig. 5b) is systematically lower when Au NPs are present (a linear trend is obtained under illumination) indicating that water oxidation is catalysed by Au NPs. This result further reinforce the catalytic role of Au NPs in water oxidation, satisfactorily explaining the increased functional performance of the TiO_2 photoanodes containing Au NPs showed in Fig. 3. Moreover, the electron conductivity through the electrodes (Fig. 5c) is also slightly improved with the presence of Au NPs, probably due to the higher electron charging of the electrode. The conductivity values extracted from EIS analysis are very similar to those reported in previous studies.[29,33] See Supplementary information, Figure S3.

Our results clearly reveal that in the studied electrodes the main contribution of the Au NPs in the mesoporous TiO_2 electrodes is catalytic. This conclusion is in good agreement with other studies showing that, in spite of the observation of the LSPR in the absorption spectra of the films, its contribution to the increase of the rupture of water and formation of H_2 is demonstrated to be negligible.[34,35] In general, although the optical gain reported for LSPR effects is relatively large, the overall enhancement of the photoconversion efficiency is still quite low, particularly in the visible region.

4. Conclusions

We have studied the photoelectrochemical behavior of TiO_2 embedded with Au NPs to photo-oxidize water. Our results show that the photoelectrodes clearly exhibit the plasmonic resonance characteristic of Au NPs. However, this optical effect is not translated into the extraction of useful photocurrent as evidenced by the spectral response evaluated by IPCE. Using impedance spectroscopy, we identify that the enhancement of the photocurrent due to the presence of Au NPs is mainly related to a catalytic effect, as evidenced by the faster hole transfer kinetics to the solution. Additionally, a slight improvement in transport properties of the film is demonstrated.

Supporting information

Includes details on EDS characterization of TiO2@Au films, impedance spectroscopy analysis of TiO2@Au films in the dark and comparison of conductivity measurements with previous studies. This material is available free of charge via the Internet.

Acknowledgements

We acknowledge the financial support of the Jaume I University (P1·1B2011-50 project). SCIC from Jaume I University is also acknowledged for instrumental facilities. Prof. Juan Bisquert is acknowledged for his constructive comments on this manuscript.

Appendix A. Supplementary data

Supplementary data associated with this article can be found, in the online version, at http://dx.doi.org/10.1016/j.electacta.2014.07.146.

References

[1] B.D. Alexander, P.J. Kulesza, L. Rutkowska, R. Solarska, J. Augustynski, Metal oxide photoanodes for solar hydrogen production, Journal of Materials Chemistry 18 (2008) 2298–2303.
[2] M.G. Walter, E.L. Warren, J.R. McKone, S.W. Boettcher, Q.X. Mi, E.A. Santori, N.S. Lewis, Solar Water Splitting Cells, Chemical Reviews 110 (2010) 6446–6473.
[3] K. Honda, A. Fujishima, Photolysis-decomposition of water at the surface of an irradiated semiconductor, Nature 238 (1972) 37.
[4] M.-C. Danel, D. Astruc, Gold nanoparticles: assembly, supramolecular chemistry, quantum-size related properties, and applicatins toward biology, catalysis, and nanotechnology, Chemical Reviews 104 (2004) 293–346.
[5] M. Haruta, Gold as a novel catalyst in the 21st century: preparation, working mechanism and applications, Gold Bulletin 37 (2004) 27–36.
[6] R. Abargues, S. Albert, J.L. Valdés, K. Abderrafi, J.P. Martínez-Pastor, Molecular-mediated assembly of silver nanoparticles with controlled interparticle spacing and chain length, Journal of Materials Chemistry 22 (2012) 22204–22211.
[7] G.L. Chiarello, E. Selli, L. Forni, Photocatalytic hydrogen production over flame spray pyrolysis-synthesised TiO2 and Au/TiO2, Applied Catalysis B: Envrionmental 84 (2008) 332–339.
[8] S.-W. Cao, Z. Yin, J. Barber, F.Y.C. Boey, S.C.J. Loo, C. Xue, Preparation of Au-BiVO4 Heterogeneous Nanostructures as Highly Efficient Visible-Light Photocatalysts, Applied Materials & Interfaces 4 (2012) 418–423.
[9] H.-Y. Lin, Y.-S. Chang, Photocatalytic water splitting for hydrogen production on Au/KTiNbO$_5$, International Journal of Hydrogen Energy 35 (2010) 8463–8471.
[10] M. Jakob, H. Levanon, P.V. Kamat, Charge distribution between UV-irradiated TiO2 and gold nanoparticles: determination of shift in the Fermi level, Nano Letters 3 (2003) 353–358.
[11] A. Takai, P.V. Kamat, Capture, store, and discharge, shuttling photogenerated electrons across TiO_2-silver interface, ACS Nano 5 (2011) 7369–7376.
[12] A. Primo, T. Marino, A. Corma, R. Molinari, H. Garcia, Efficient visible-light photocatalytic water splitting by minute amounts of gold supported on nanoparticulate CeO2 obtained by a bioploymer templating method, Journal of American Chemical Society 133 (2011) 6930–6933.
[13] Z. Liu, W. Hou, P. Pavaskar, M. Aykol, S.B. Cronin, Plasmon resonant enhancement of photocatlytic water splitting under visible illumination, Nano Letters 11 (2011) 1111–1116.
[14] L. Du, A. Furube, K. Yamamoto, K. Hara, R. Katoh, M. Tachiya, Plasmon-induced charge separation and recombination in gold-TiO_2 nanoparticle systems: dependence of TiO_2 particle size, The Journal of Physical Chemistry C 113 (2009) 6454–6462.
[15] A. Furube, L. Du, K. Hara, R. Katoh, M. Tachiya, Ultrafast plasmon-induced electron transfer from gold nanodots into TiO2 nanoparticles, Journal of American Chemical Society 129 (2007) 14852–14853.
[16] Y. Tian, T. Tatsuma, Plasmon-induced photoelectrochemistry at metal nanoparticles supported on nanoporous TiO_2, Chemical Communications 40 (2004) 1810–1811.
[17] Y.-W. Tai, J.-S. Chen, C.-C. Yang, B.-Z. Wan, Preparation of nano-gold on K2La2Ti3O10 for producing hydrogen from photo-catalytic water splitting, Catalysis Today 97 (2004) 95–101.
[18] Y. Tian, T. Tatsuma, Mechanism and applications of plasmon-induced charge separation at TiO_2 films loades with gold nanoparticles, Journal of American Chemical Society 127 (2005) 7632–7637.
[19] W. Hou, S.B. Cronin, A review of surface plasmon resonance-enhanced photocatalysis, Advanced Functional Materials 23 (2013) 1612–1619.
[20] D.B. Ingram, S. Linic, Water splitting on composite plasmonic-metal/semiconductor photoelectrodes: evidence for selective plasmon-induced formation of charge carriers near the semiconductor surface, Journal of American Chemical Society 133 (2011) 5202–5205.
[21] B. Iandolo, T.J. Antosiewicz, A. Hellman, I. Zoric, On the mechanism for nanoplasmonic enhancement of photon to electron conversion in nanoparticle sensitized hematite films, Phys. Chem. Chem. Phys. 15 (2013) 4947–4954.
[22] H. Wang, T. You, W. Shi, J. Li, L. Guo, Au/TiO_2/Au as a plasmonic coupling photocatalyst, The Journal of Physical Chemistry C 116 (2012) 6490–6494.
[23] S. Mubeen, G. Hernandez-Sosa, D. Moses, J. Lee, M. Moskovits, Plasmonic photosensitization of a wide band gap semiconductor; converting plasmons to charge carriers, Nano Letters 11 (2011) 5548–5552.
[24] J. Lee, S. Mubeen, X. Ji, G.D. Stucky, M. Moskovits, Plasmonic photoanode for solar water splitting with visible light, Nano Letters 12 (2012) 5014–5019.
[25] M.D. Brown, T. Suteewong, R.S.S. Kumar, V. D'Innocenzo, A. Petrozza, M.M. Lee, U. Wiesner, H. Snaith, Plasmonic Dye-Sensitized Solar Cells Using Core-Shell Metal-Insulator Nanoparticles, Nano Letters 11 (2011) 438–445.
[26] P. Garcia de Arquer, A. Mihi, D. Kufer, G. Konstantatos, Photoelectric Energy COnversion of Plasmon-Generated Hot Carriers in Metal-Insulator-Semiconductor Strucutres, ACS Nano 7 (2013) 3581–3588.
[27] T. Berger, T. Lana-Villarreal, D. Monllor-Satoca, R. Gomez, An electrochemical study on the nature of trap states in nanocrystalline rutile thin films, Journal of Physical Chemistry C 111 (2007) 9936–9942.
[28] H.L. Wang, J.J. He, G. Boschloo, H. Lindstrom, A. Hagfeldt, S.E. Lindquist, Electrochemical investigation of traps in a nanostructured TiO2 film, Journal of Physical Chemistry B 105 (2001) 2529–2533.
[29] S. Gimenez, H.L. Dunn, P. Rodenas, F. Fabregat-Santiago, S.G. Miralles, E.M. Barea, R. Trevisan, A. Guerrero, J. Bisquert, Carrier density and interfacial kinetics of mesoporous TiO2 in aqueous electrolyte determined by impedance spectroscopy, Journal of Electroanalytical Chemistry 668 (2012) 119–125.

[30] J. Ran, J. Zhang, J. Yu, M. Jaroniec, S.Z. Qiao, Earth-abundant cocatalysts for semiconductor-based photocatalytic water splitting, Chemical Society Reviews (2014), http://dx.doi.org/10.1039/C3CS60425J.
[31] J. Bisquert, Theory of the impedance of electron diffusion and recombination in a thin layer, Journal of Physical Chemistry B 106 (2002) 325–333.
[32] Y. Nakato, K. Abe, H. Tsubomura, New photovoltaic effect observed for metal-coated semiconductor electrodes and its utilization for photolysis of water, Berichte Der Bunsen-Gesellschaft-Physical Chemistry Chemical Physics 80 (1976) 1002–1007.
[33] P. Rodenas, T. Song, P. Sudhagar, G. Marzari, H. Han, L. Badia-Bou, S. Gimenez, F. Fabregat-Santiago, I. Mora-Sero, J. Bisquert, U. Paik, Y.S. Kang, Quantum Dot Based Heterostructures for Unassisted Photoelectrochemical Hydrogen Generation, Advanced Energy Materials 3 (2013) 176–182.
[34] W.-H. Tu, Y.-K. Hsu, C.-H. Yen, C.-I. Wu, J.-S. Hwang, L.-C. Chen, K.-H. Chen, Au nanoparticle modified GaN photoelectrode for photoelectrochemical hydrogen generation, Electrochemistry Communications 13 (2011) 530–533.
[35] S.V. Awate, S.S. Deshande, K. Rakesh, P. Dhanasekaran, N.M. Gupta, Role of micro-structure and interfacial properties in the higher photocatalytic activity of TiO2-supported nanogold for methanol-assisted visible-light.induced splitting of water, Phys. Chem. Chem. Phys. 13 (2011) 11329–11339.